Interannual Variability of the Asian Summer Monsoon: Contrasts between the Indian and the Western North Pacific–East Asian Monsoons*

BIN WANG

Department of Meteorology and International Pacific Research Center, University of Hawaii at Manoa, Honolulu, Hawaii

RENGUANG WU

International Pacific Research Center, University of Hawaii at Manoa, Honolulu, Hawaii

K.-M. LAU

Climate and Radiation Branch, NASA Goddard Space Flight Center, Greenbelt, Maryland

(Manuscript received 28 July 2000, in final form 10 April 2001)

ABSTRACT

Analyses of 50-yr NCEP–NCAR reanalysis data reveal remarkably different interannual variability between the Indian summer monsoon (ISM) and western North Pacific summer monsoon (WNPSM) in their temporal–spatial structures, relationships to El Niño, and teleconnections with midlatitude circulations. Thus, two circulation indices are necessary, which measure the variability of the ISM and WNPSM, respectively. A weak WNPSM features suppressed convection along 10°–20°N and enhanced rainfall along the mei-yu/baiu front. So the WNPSM index also provides a measure for the east Asian summer monsoon. An anomalous WNPSM exhibits a prominent meridional coupling among the Australian high, cross-equatorial flows, WNP monsoon trough, WNP subtropical high, east Asian subtropical front, and Okhotsk high. The WNP monsoon has leading spectral peaks at 50 and 16 months, whereas the Indian monsoon displays a primary peak around 30 months. The WNPSM is weak during the *decay* of an El Niño, whereas the ISM tends to abate when an El Niño *develops*. Since the late 1970s, the WNPSM has become more variable, but its relationship with El Niño remained steady; in contrast, the ISM has become less variable and its linkage with El Niño has dramatically declined. These contrasting features are in part attributed to the differing processes of monsoon–ocean interaction.

Also found is a teleconnection between a suppressed WNPSM and deficient summer rainfall over the Great Plains of the United States. This boreal summer teleconnection is forced by the heat source fluctuation associated with the WNPSM and appears to be established through excitation of Rossby wave trains and perturbation of the jet stream that further excites downstream optimum unstable modes.

1. Introduction

The Asian summer monsoon is one of the most energetic components of the earth's climate system. Prediction of its interannual variation is among the most imperative tasks in climate research and climate forecast. Before the 1990s, studies and forecasts of the Asian summer monsoon variability have focused on local scales, for an individual country or a particular region, for example. Webster and Yang (1992) first attempted to quantify year-to-year variations of the broadscale Asian summer monsoon using the vertical shear averaged over the south Asian region. Whether it is appropriate to use a single indicator such as the Webster and Yang index to measure the Asian summer monsoon variability has been a controversial issue (Goswami et al. 1999; Wang and Fan 1999). Wang and Fan (1999) found that the two major convective heat sources that drive the Asian summer monsoon—the convection over the Bay of Bengal–India–Arabia Sea and that over the South China Sea and Philippine Sea—are poorly correlated on interannual timescales. Thus, they advocate use of two, rather than one, indices to quantify the variability of the Asian summer monsoon.

Previous studies of the variability of the Asian summer monsoon mainly focused on the Indian summer monsoon (ISM) and east Asian summer monsoon (EASM). The relationship between the ISM and South-

* School of Ocean and Earth Science and Technology Publication Number 5806 and International Pacific Research Center Publication Number 99.

Corresponding author address: Prof. Bin Wang, International Pacific Research Center, School of Ocean and Earth Science and Technology, University of Hawaii at Manoa, 2525 Correa Rd., Honolulu, HI 96822-2219.
E-mail: bwang@soest.hawaii.edu

ern Oscillation noticed by Walker (1923, 1924) has received renewed interest in the last two decades (e.g., Rasmusson and Carpenter 1983; Shukla and Paolino 1983; Mooley and Shukla 1987; Yasunari 1990; Webster and Yang 1992; Lau and Yang 1996; Ju and Slingo 1995; Soman and Slingo 1997; Liu and Yanai 2001; Lau and Nath 2000, among many others). The tantalizing ISM–ENSO (El Niño–Southern Oscillation) relation has experienced secular changes (e.g., Webster et al. 1998 and references therein; Kripalani and Kulkarni 1997a; Krishnamurthy and Goswami 2000), especially in the last four decades (Shukla 1995; Kumar et al. 1999). The interannual variation of the EASM has also been intensively investigated (Nitta 1987; Huang and Wu 1989; Tao and Chen 1987; Lau 1992; Chen et al. 1992; Shen and Lau 1995; Ye and Huang 1996; Zhang et al. 1996; Weng et al. 1999; Chen and Yoon 2000; Lau et al. 2000, among others).

In contrast to the ISM and EASM, the western North Pacific summer monsoon (WNPSM) variability has been a research-void area. Only recently, Wu and Wang (2000) investigated the cause of the interannual variation of the WNPSM onset. However, compared to the ISM, the WNPSM has not only more pronounced year-to-year variability but also more profound impacts on the EASM and ENSO. Nitta (1987) and Huang and Wu (1989) found that rainfall anomalies associated with the mei-yu/baiu front are correlated with variations of the convective activity over the Philippine Sea. Based on a study of the strong ENSO episodes in the last 50 yr, Wang et al. (2000) found that a key system linking the Pacific warming and the east Asian climate is an anomalous anticyclone in the subtropical WNP. The anticyclone establishes during mature phases of warm episodes and lasts through the ensuing early summer, exerting a prolonged impact of ENSO on the EASM. Chang et al. (2000) also stressed the influences on the EASM from the anomalous 850-hPa anticyclone near the southeast coast of China during spring and early summer. The WNP wind anomalies and associated equatorial zonal wind anomalies were shown to play active roles in the thermocline adjustment associated with ENSO cycle, which has a direct feedback to the turnabout of ENSO (Wang et al. 1999).

The above review suggests the importance of understanding the monsoon variability over the WNP and its interaction with ENSO. The present study is aimed at a methodical documentation of the WNPSM variability. While emphasizing the WNPSM, we are also particularly concerned with the differences in the interannual variations between the ISM and WNPSM, as well as their relations with ENSO, EASM, and midlatitude climate anomalies.

The data used in the present analysis are derived from a 50-yr (1948–97) National Centers for Environmental Prediction–National Center for Atmospheric Research reanalysis. Details of the data were documented by Kalnay et al. (1996). Monthly mean rainfall data on a 2.5° × 2.5° grid are obtained from the Climate Prediction Center (CPC) Merged Analysis of Precipitation (CMAP), spanning the period from January 1979 to December 1997 (Xie and Arkin 1997). We used the version derived by merging rain gauge observations with rainfall estimates inferred from various satellite observations but *without* numerical model outputs. To focus on interannual variations, the monthly mean anomalies are decomposed into interannual and interdecadal components. The former is simply represented by the Fourier harmonics with periods ranging from 2 to 8 yr, while the latter contains all harmonics with periods longer than 8 yr. Throughout the paper, we use the interannual component of the data.

To contrast the variability of the ISM and WNPSM, we will first define two monsoon indices originally proposed by Wang and Fan (1999) based on theoretical considerations and empirical relationships between the lower-tropospheric winds and two major convective heat sources that drive the Asian summer monsoon (section 2). Such defined indices are demonstrated to represent respectively the dominant modes of the ISM and WNP–EASM variability. Sections 3 and 4 compare, respectively, the temporal and spatial structures of the ISM and WNPSM. Section 5 depicts statistically significant teleconnection patterns associated with a strong-minus-weak ISM and WNPSM. Lag correlation analysis is used to contrast their relationships with ENSO (section 6). Section 7 discusses possible mechanisms responsible for the differences in the variability of the ISM and WNPSM. The last section summarizes major conclusions.

2. Dynamic indices for the Indian and western North Pacific summer monsoons

The Asian summer monsoon is primarily driven by convective, radiative, and sensible heat sources/sinks, among which convective latent heating is most important. During boreal summer, the most intense convection is observed over two regions: the Bay of Bengal–India–Arabian Sea and the South China Sea–Philippine Sea. The centers of the two convection regions exhibit distinctive annual excursions (Fig. 1). Over the Indian Ocean, the monthly mean maximum rainfall is anchored west of Sumatra (5°S, 100°E) from September to March. In May, the convection center crosses the equator, moving into the southern Bay of Bengal (5°N, 92°E). From May to June, heavy rainfall area jumps northward to the head of Bay of Bengal and remains there throughout the rest of summer. In contrast to this bifocal annual march, the convection center in the western Pacific shows an elongated round-trip excursion between Solomon Island (5°S, 165°E) (during Dec–Mar) and the Philippine Sea (during Jun–Oct). From April to November, the western Pacific convection center displays an overriding east–west movement from 165° to 125°E.

The heat sources over the Bay of Bengal and Phil-

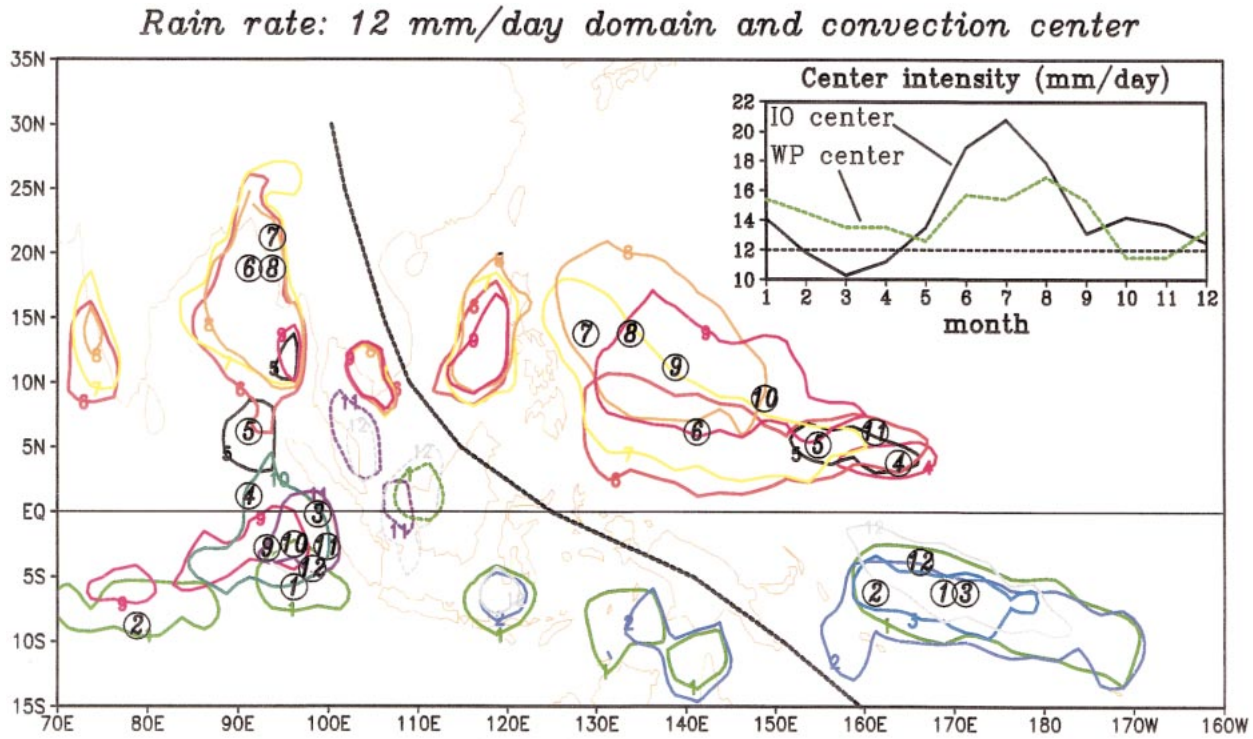

FIG. 1. Annual march of the rain-rate centers over the Indian and the western Pacific Oceans. The contours denote rain rate of 12 mm day^{-1}. The locations of the maximum rain rate are indicated by circled bold italic. Intensities of the monthly mean maximum rain rate for the two centers are given in the plot at the upper-right corner.

ippine Sea affect, respectively, the ISM and WNPSM, because well-defined wind anomalies occur over and to the west of the convective heat sources as a Rossby wave response to the latent heat released in the two convection regions (Matsuno 1966; Gill 1980). Wang and Fan (1999) found that the correlation between interannual variations of the south Asian and WNP convection is statistically *insignificant*. Thus, they recommended use of two indices to measure the variability of the ISM and WNPSM, respectively. Rainfall anomalies averaged over the core regions of the ISM and WNPSM (shown in Fig. 2) are meaningful indices, yet the rainfall data (CMAP) have a limited length. To obtain a longer time series, corresponding circulation indices are desirable. To choose a circulation index dynamically consistent with convective heating, we focus on 850-hPa winds. This is because 850-hPa wind variations reflect variations of corresponding convective heating better than the upper-level circulation or vertical shear (Wang 2000) and the 850-hPa vorticity is highly indicative of the strength of boundary layer moisture convergence and rainfall in regions away from the equator.

A dynamic index for the ISM is defined using the difference of the 850-hPa zonal winds between a southern region of 5°–15°N, 40°–80°E and a northern region of 20°–30°N, 70°–90°E (indicated by the two solid-line boxes near India in Fig. 2). We do not choose the vorticity itself because the meridional wind shear has a weaker correlation with the rainfall and the zonal wind part dominates in the vorticity. In addition, such defined index reflects both the intensity of the tropical westerly monsoon and the lower-tropospheric vorticity anomalies associated with the ISM trough. Hereafter it is referred to as the Indian monsoon index (IMI). The IMI not only represents well the rainfall anomalies averaged over an extended region including the Bay of Bengal, India, and the eastern Arabian Sea, it is also highly correlated with the all-India summer rainfall (Parthasarathy et al. 1992) with a correlation coefficient of 0.72 for the 50-yr period from 1948 to 1997.

The dynamic monsoon index for the WNPSM (hereafter the WNP monsoon index or WNPMI) was defined, following Wang and Fan (1999), as the difference of 850-hPa westerlies between a southern region (5°–15°N, 100°–130°E) and a northern region (20°–30°N, 110°–140°E; Fig. 2). This latitudinal differential westerly index reflects not only the strength of the tropical westerlies but also the intensity of the low-level vorticity associated with the Rossby wave response to the Philippine Sea convective heat source.

The IMI and WNPMI represent the dominant modes of interannual variations of the ISM and WNPSM, respectively. To substantiate this assertion, we applied multivariate EOF analysis to the 850-hPa anomalous zonal and meridional wind components for the period of 1948–97. In the ISM domain, the leading EOF mode,

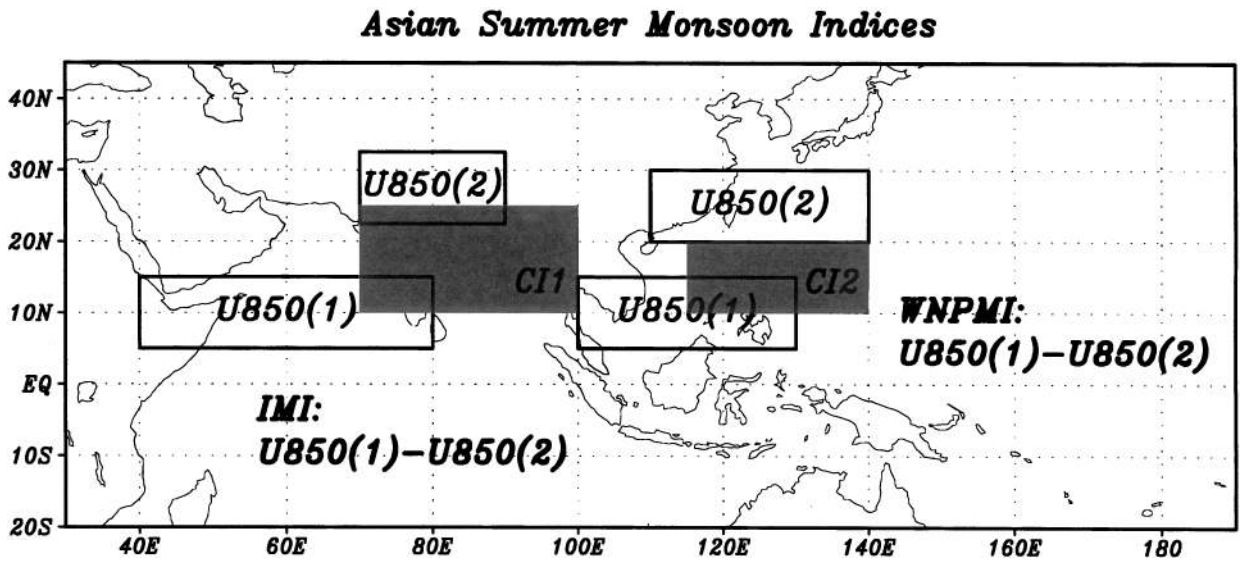

FIG. 2. Schematic diagram for the definition of the monsoon circulation indices, IMI and WNPMI. Shaded boxes indicate the regions for the rainfall indices, CI1 and CI2. The solid boxes denote regions where the zonal winds are used to define the monsoon circulation indices (refer to the text for details).

which accounts for about 20% of the total variance, displays that the ISM trough and associated anomalous westerlies between 5° and 20°N and easterlies over northern India are enhanced (Fig. 3a). The time coefficient of this mode positively correlates with the IMI with a correlation coefficient of 0.73 for the 40-yr period from 1958 to 1997 (Fig. 3b).

In the WNP–EASM domain, the leading EOF mode enlightens about 22% of the total variance. During a strong WNPSM, an anomalous cyclone elongated along 20°N dictates the WNP (Fig. 4a). Westerly anomalies prevail between 5° and 15°N and easterly anomalies between 20° and 30°N. An anomalous anticyclonic ridge is found around 35°N extending from the central Pacific to eastern China and Japan. The corresponding time coefficient of the first EOF mode correlates highly with the WNPMI (the correlation coefficient is 0.88 for the 50-yr period; Fig. 4b). Thus, the WNPMI reflects faithfully the dominant mode of the lower-level wind anomaly over the WNP–EASM. The anomalous circulation patterns shown in Fig. 4a indicate that the WNP monsoon trough and the western Pacific subtropical high fluctuate in a coherent manner. As such, they, along with the subtropical monsoon front (north of the western Pacific subtropical high), form an integrated monsoon circulation system. In this sense, the WNPMI portrays not only the variation of the WNPSM but also, to a certain extent, that of the EASM.

For the period of 1948–97, the correlation between the IMI and WNPMI (0.17) is statistically insignificant at the 95% confidence level; the correlation between the IMI and the time coefficient of the leading WNP–EASM mode is negligibly small (0.05). These results corroborate with the conclusion of Wang and Fan (1999) who derived their conclusion based on a shorter period (1975–97) of outgoing longwave radiation data.

3. Temporal structures of the variability of the two monsoon subsystems

There are two important differences between the temporal evolution of the ISM and WNPSM. First, the standard deviation of the WNPMI (1.72) is twice that of the IMI (0.87). Hence, the WNPSM is much more variable than the ISM. Second, the amplitude of WNPMI has increased significantly since 1980 (Fig. 4b), while the IMI displays a decreased variability in the last two decades (Fig. 3b). During the 1970s, however, the ISM exhibited large variability while the WNPSM variability was moderate. This implies an out-of-phase tendency in interdecadal modulations of the interannual variability of the ISM and WNPSM.

More interestingly, power spectrum analysis of monthly mean time series of IMI and WNPMI discloses differing dominant periodicities of the Indian and WNP monsoons. The spectrum of the IMI has a leading energy peak at a period of 30 months (Fig. 5a), indicating a quasi-biennial rhythm in the Indian monsoon. The spectrum of the WNP monsoon, on the other hand, shows a prominent peak at 50 months, while the peak in the quasi-biennial timescale (26 months) is barely significant at the 90% confidence level (Fig. 5b). The WNP monsoon also has a distinctive peak at 16 months. A similar spectral peak was found in a number of previous studies. Yanai and Li (1994) found peaks near 15 months in the Webster and Yang index, Eurasian snow cover, and equatorial eastern Pacific SST. Jiang et al. (1995) found a 15-month peak in the equatorial eastern Pacific

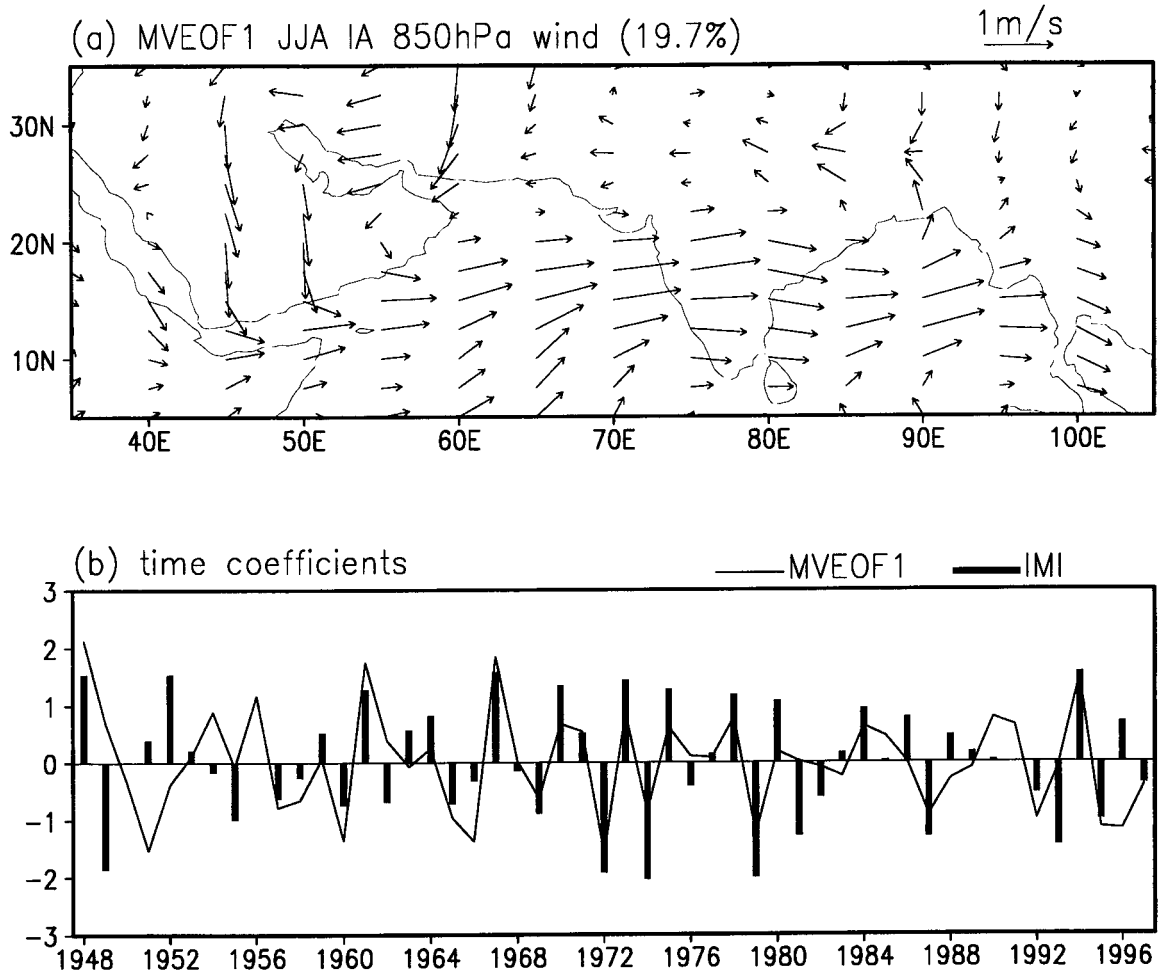

FIG. 3. (a) The leading multivariate EOF mode and (b) time coefficient of 850-hPa winds in the south Asian monsoon region for summer of 1948–97. The wind scales are displayed at the upper-right corners of (a) and (b). For comparison, the normalized IMI is plotted in (b) using bar charts.

SST. Wang et al. (1999) found that the surface wind stress curl over the Philippine Sea has a pronounced spectral peak at 16 months. No explanation has been offered concerning the origin of this 15–16-month energy peak. It certainly deserves further investigation, but that is beyond the scope of the current paper.

Persistence and periodicity can be seen from the time series of composite IMI and WNPMI for strong and weak monsoon years (Fig. 6). The strong and weak monsoon years are selected based on the IMI and WNPMI. The years with a monsoon index greater (less) than one standard deviation were tagged as strong (weak) monsoon years. For the composite weak ISM, a discernible persistency is seen from the preceding spring to summer. No precursory signals are found in the preceding winter. The index, however, shows a reversal of sign in July of one year before and after (Fig. 6a), indicating a tendency toward a biennial cycle. This is consistent with the spectral analysis (Fig. 5a; Goswami et al. 1999; Tomita and Yasunari 1996). The composite temporal evolution of area-mean rainfall over south Asia shows a similar reversal. The biennial tendency is particularly evident for the composite weak monsoon, that is, *a weak ISM tends to be preceded and followed by a strong ISM*. For the WNPSM, a weak persistent tendency in the preceding spring is detectable for the composite strong monsoon, but not for the composite weak monsoon (Fig. 6b). The tendency of biennial variation is insignificant, which also agrees with the spectral analysis (Fig. 5b).

4. Spatial structures of the variability of the two Asian monsoon subsystems

To contrast the spatial structures of monsoon variability, we present composite maps of strong-minus-weak ISM and WNPSM years, respectively. In general, the anomalies associated with the strong and weak monsoon tend to have opposite polarities. Thus, the composite strong-minus-weak monsoon will be simply re-

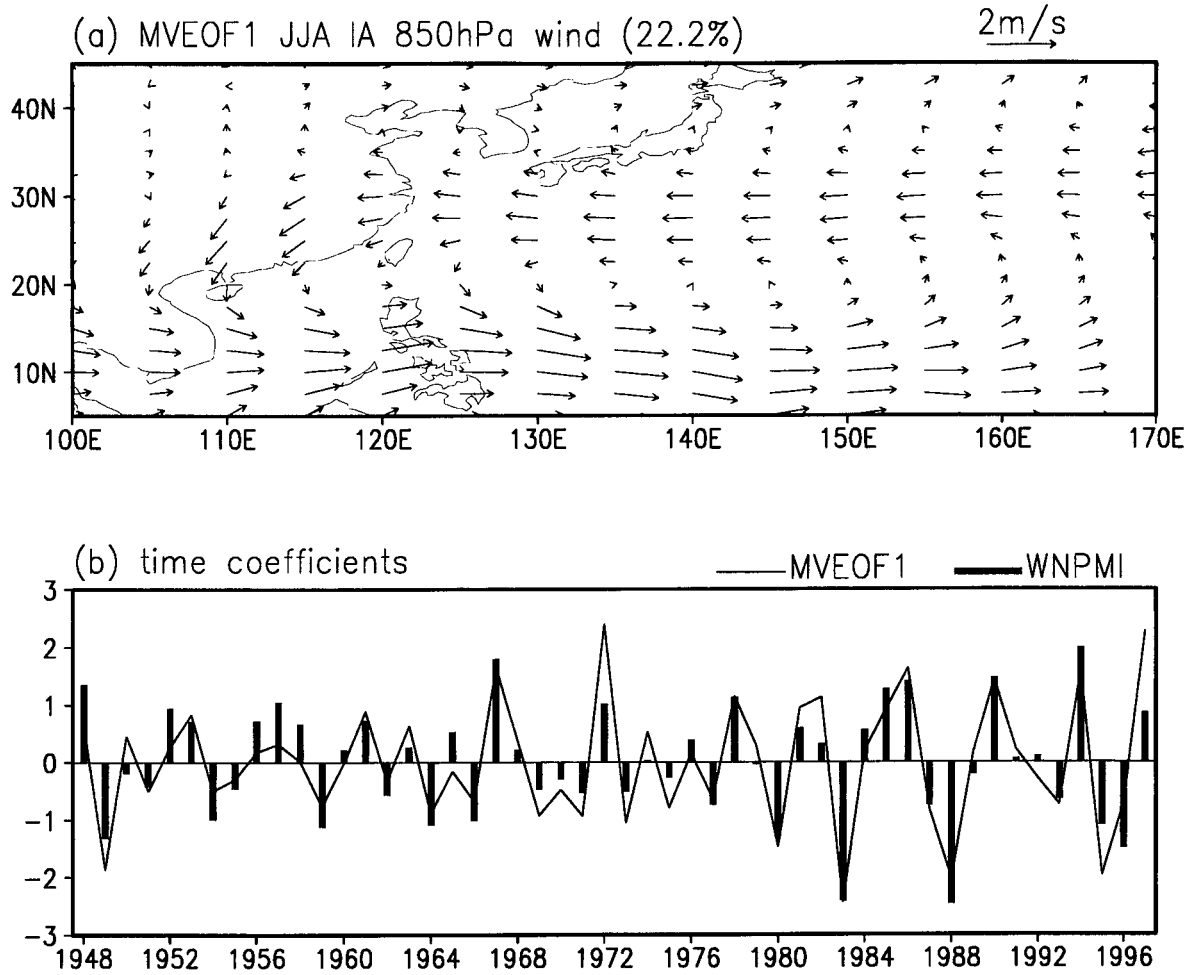

FIG. 4. The same as Fig. 3 except for the western North Pacific–east Asian monsoon region and the WNPMI.

ferred to as strong monsoon anomalies. Correlation or regression maps with reference to the monsoon indices yield very similar results.

During a strong ISM, the rainfall increases over the core region of the ISM (Fig. 7a). The composite rainfall difference attains a 95% confidence level in northeast India. Corresponding to the increased rainfall of the ISM, significant monsoon circulation anomalies are primarily confined to the region west of 90°E (Fig. 8). At 200 hPa, both the south Asian high and Mascarene high and the easterly winds in between are enhanced (Fig. 8a). At 850 hPa, a clockwise monsoon gyre consisting of easterlies in subtropical south Indian Ocean, cross-equatorial southerlies along the east African coast, and westerlies extending from the east African coast to the Bay of Bengal is enhanced (Fig. 8c). This gyre connects enhanced Mascarene high and Indian monsoon trough. The low-level wind composite based on all-Indian summer rainfall (Annamalai et al. 1999) shows quite similar features though noticeable differences are found in the equatorial Indian Ocean and WNP. The strong-minus-weak monsoon pattern shown in Fig. 8 supports the notion of the ISM circulation systems proposed by Krishnamurti and Bhalme (1976). The barotropic structure over the Tibetan Plateau suggests that the high-pressure anomalies are likely generated by sensible heat flux associated with the prominent positive surface temperature anomalies (Fig. 7b).

In contrast, during a strong WNPSM, rainfall increases significantly in a zonally oriented band along 10°–20°N extending from the South China Sea to the central North Pacific (Fig. 9a). Negative rainfall anomalies are found over the east Asian subtropical monsoon front extending from the lower reaches of the Yangtze River valley to the east of Japan, indicating an out-of-phase variation between the WNP and mei-yu/baiu rainfall. Another suppressed convection zone extends from Borneo northwestward to the southeast Arabian Sea. In correspondence with the rainfall anomalies over the WNP shown in Fig. 9a, pronounced 200-hPa divergent flows are found in the WNP along 20°N and connect with the northeasterly cross-equatorial flows over the Maritime Continent and the enhanced Australian high (Fig. 10a). The 850-hPa westerly anomalies prevailing over the

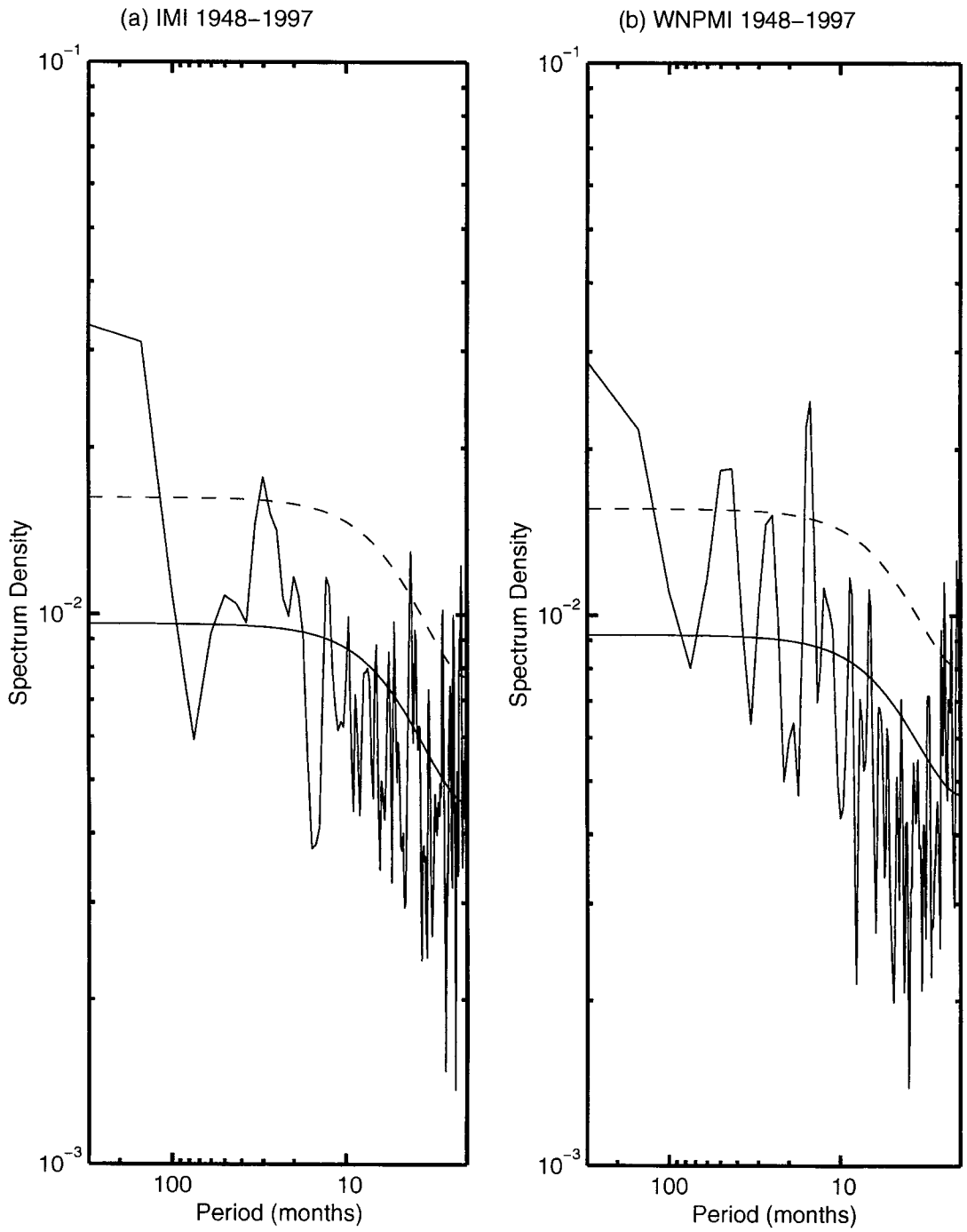

FIG. 5. Spectra of the monthly mean (a) IMI and (b) WNPMI for the period of 1948–97. The smooth solid and dashed curves are for the red noise spectrum and its 90% confidence level.

Philippine Sea are linked with westerlies over the equatorial western-central Pacific and cross-equatorial southerly flows west of Sumatra (Fig. 10c). In the lower and midtroposphere, alternative cyclonic and anticyclonic anomalies are found along 20° and 35°N, respectively (Figs. 10b,c).

These zonally elongated cyclones and anticyclone extend from 110°E to the date line. They are, respectively, aligned with the underlying negative and positive SST anomalies in the North Pacific (Fig. 9b). If the SST anomalies are controlled by surface heat fluxes (it is likely the case in the midlatitudes during summer), the observed SST anomalies may be a result of the atmospheric forcing associated with cloudiness and surface

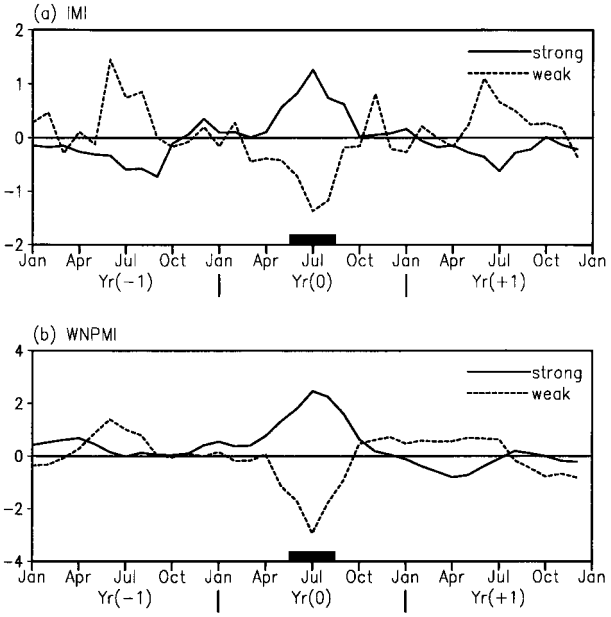

FIG. 6. Composite temporal evolution of the monthly mean (a) IMI and (b) WNPMI for strong and weak monsoons from the year before (−1) to the year after (+1) the summer monsoon.

winds. To what extent the SST anomalies feed back to the atmosphere is an interesting question to be investigated. The surface temperature, precipitation, and circulation anomalies all display prominent longitudinal band structures in the east Asia and WNP region. These anomalies imply northward displacement of the WNP monsoon trough, the WNP subtropical high, and westerly jet stream during a strong WNPSM.

5. Teleconnections associated with anomalous WNP and Indian summer monsoons

The teleconnection associated with a strong ISM exhibits two noteworthy features. The first is previously seen in the eastern Pacific. During a strong ISM, the South Pacific subtropical high is enhanced. Along the equator, 850-hPa easterlies and 200-hPa westerlies prevail, which are associated with anomalous subsidence induced by the negative SST anomalies in the equatorial eastern Pacific (Fig. 7b). This verifies the finding of Webster and Yang (1992) with a much longer dataset. Another notable, statistically significant teleconnection links the EASM and ISM: a prominent anticyclonic anomaly is found over northeast China (Fig. 8). This pattern would imply an increased rainfall over northern China and reduced rainfall over Japan. Enhanced rainfall over northern China in association with excessive Indian rainfall was indicated in previous studies (Tao and Chen 1987; Guo and Wang 1988; Kripalani and Singh 1993; Kripalani and Kulkarni 1997b; Zhang et al. 1999). What causes and maintains this equivalent barotropic anticyclonic anomaly? It is important to note that this anomalous anticyclone is associated with pronounced positive SST anomalies in the east Asian marginal seas (Yellow Sea, East China Sea, and Japan Sea) and the Kuroshio extension (Fig. 7b). Presumably, the anomalous anticyclone would reduce the cloud cover and increase the downward solar radiation. To the southeast of the anticyclonic anomaly, the total wind speed would decrease because the mean surface winds are southwesterlies. The decrease of the total wind speed would reduce the surface latent heat loss. Both above two processes favor ocean surface warming. On the other hand, the warming might in turn reinforce the anticyclonic anomalies by enhancing upward sensible heat flux. Since the heating associated with the sensible heat flux decreases upward, it facilitates the generation of a barotropic atmospheric response and favors an anomalous high above the surface warming. Thus, the anticyclone and the underlying SST anomalies might maintain themselves through the above-mentioned positive feedback between ocean and atmosphere.

The teleconnection associated with anomalous WNPSM is more remarkable in terms of its extent and intensity. During a strong WNPSM, a pronounced wave train pattern, seen in the lower, mid-, and upper troposphere, emanates from the WNP, crosses the North Pacific and extends to North America (Fig. 10). The wave train consists of five major cells. They are, respectively, an east–west elongated cyclone along 20°N in the subtropical WNP off the coast of east Asia, an elongated anticyclone along 35°N extending from the Yellow Sea to the date line, an elongated cyclone extending from the Okhotsk Sea to the Bering Sea, an anticyclone over the Gulf of Alaska and northwestern Canada, and a cyclone over the Great Lakes of North America. At 500 hPa, the wave train pattern matches well with the low-level height anomalies implied by the 850-hPa wind anomalies (Figs. 10b,c). The wave train exhibits a dominant barotropic structure north of 30°N. However, in the Tropics between 10° and 30°N where the wave train originated, the circulation exhibits a baroclinic structure with a cyclone at 850 and 500 hPa capped by 200-hPa divergent flows (Fig. 10).

The summer wave train depicted in Fig. 10 suggests a linkage between the climate anomalies over North America and the WNP. A weak WNPSM (suppressed convection in the WNP) implies an anomalous cyclone located in the Gulf of Alaska and northwest Canada (centered at 55°N, 130°W) and an anomalous anticyclone over the Great Lakes (50°N, 90°W). The latter corresponds to a deficient summer rainfall in the Great Plains. The wind and height patterns over the North American sector for a composite strong-minus-weak WNPSM are very similar to the 500-hPa wind difference between wet and dry Great Plains years shown by Ting and Wang (1997, their Fig. 11c). It implies that a weak WNPSM tends to be correlated with an anomalous high pressure over the Great Lakes and below-normal precipitation in the Great Plains (32°–45°N, 105°–

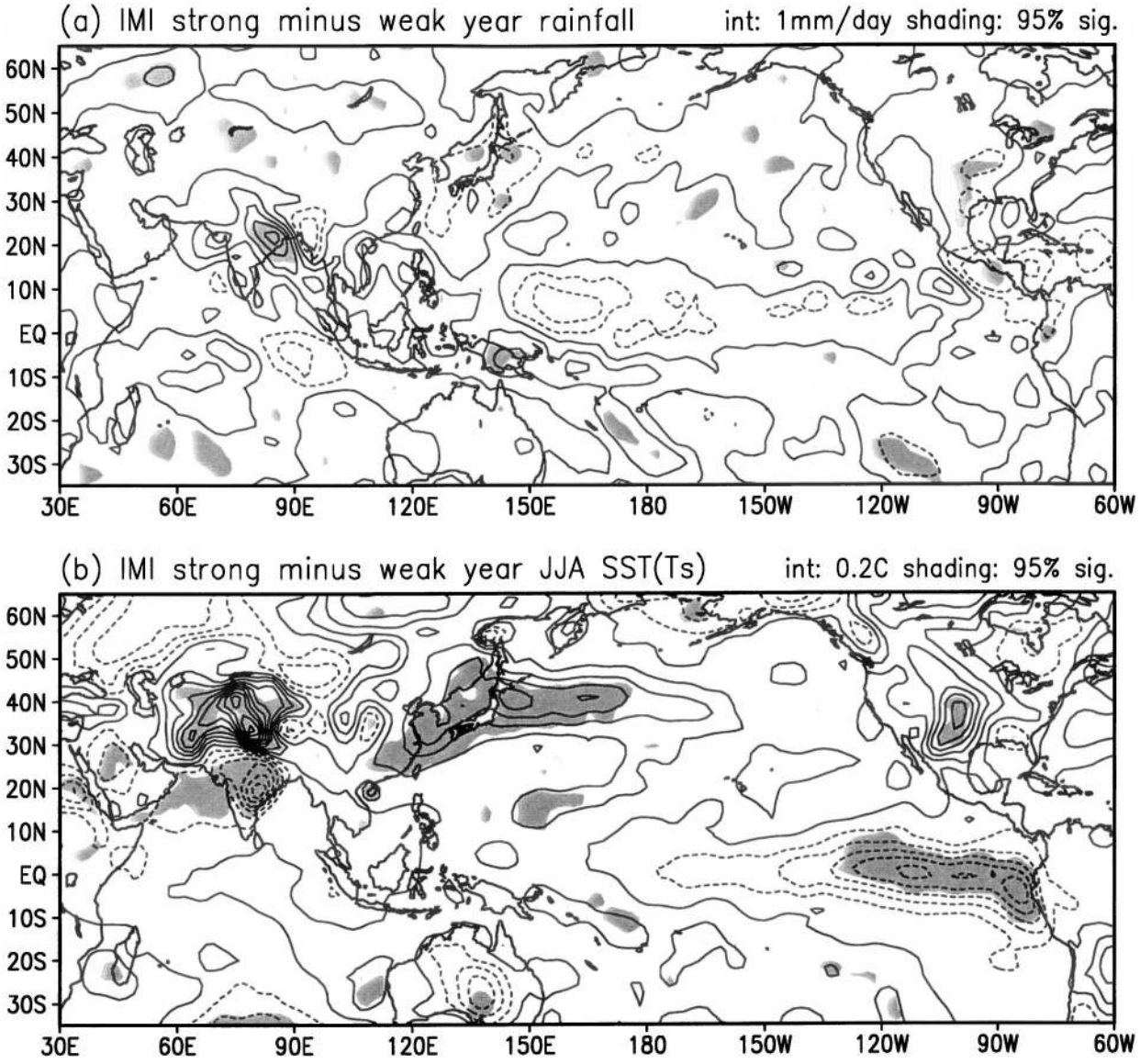

FIG. 7. Composite difference of (a) summer rainfall and (b) sea (land) surface temperature between the strong and weak monsoon years with respect to the IMI. The contour interval is 1 mm day^{-1} for the rainfall and 0.2°C for SST. Shading denotes regions of difference at 95% confidence level. The rainfall data cover 1979–96 only.

85°W). Using the 50-yr (1948–97) data, we constructed a seasonal mean [Jun–Aug (JJA)] WNPMI without time filtering, that is, the seasonal anomalies contain both interannual and decadal variations. A significant correlation coefficient (0.42) was found between the WNPMI and the U.S. Great Plains precipitation index used by Ting and Wang (1997). In particular, there were eight weak WNPSM years (1954, 1955, 1959, 1966, 1983, 1988, 1995, and 1996), during which, the summer rainfall over the Great Plains was *all* deficient, including the three most severe droughts (1976, 1983, and 1988, Ting and Wang 1997).

The summer teleconnection between the WNP–east Asia and North America is an important yet intriguing phenomenon. Since the teleconnection pattern is directly related to the fluctuation of the heat source over the WNP, it is likely that the variability of the WNPSM has an influence on the North American climate. In a recent study, Lau and Weng (2001) revealed a teleconnection with reference to U.S. droughts and floods that links to the Asian–Pacific monsoon anomalies. Here we showed evidence that the WNPSM variation has a remote response over North America. We speculate that the WNP heat source may affect the North American climate via two mechanisms. One is through the heating-induced meridional circulation that perturbs midlatitude jet

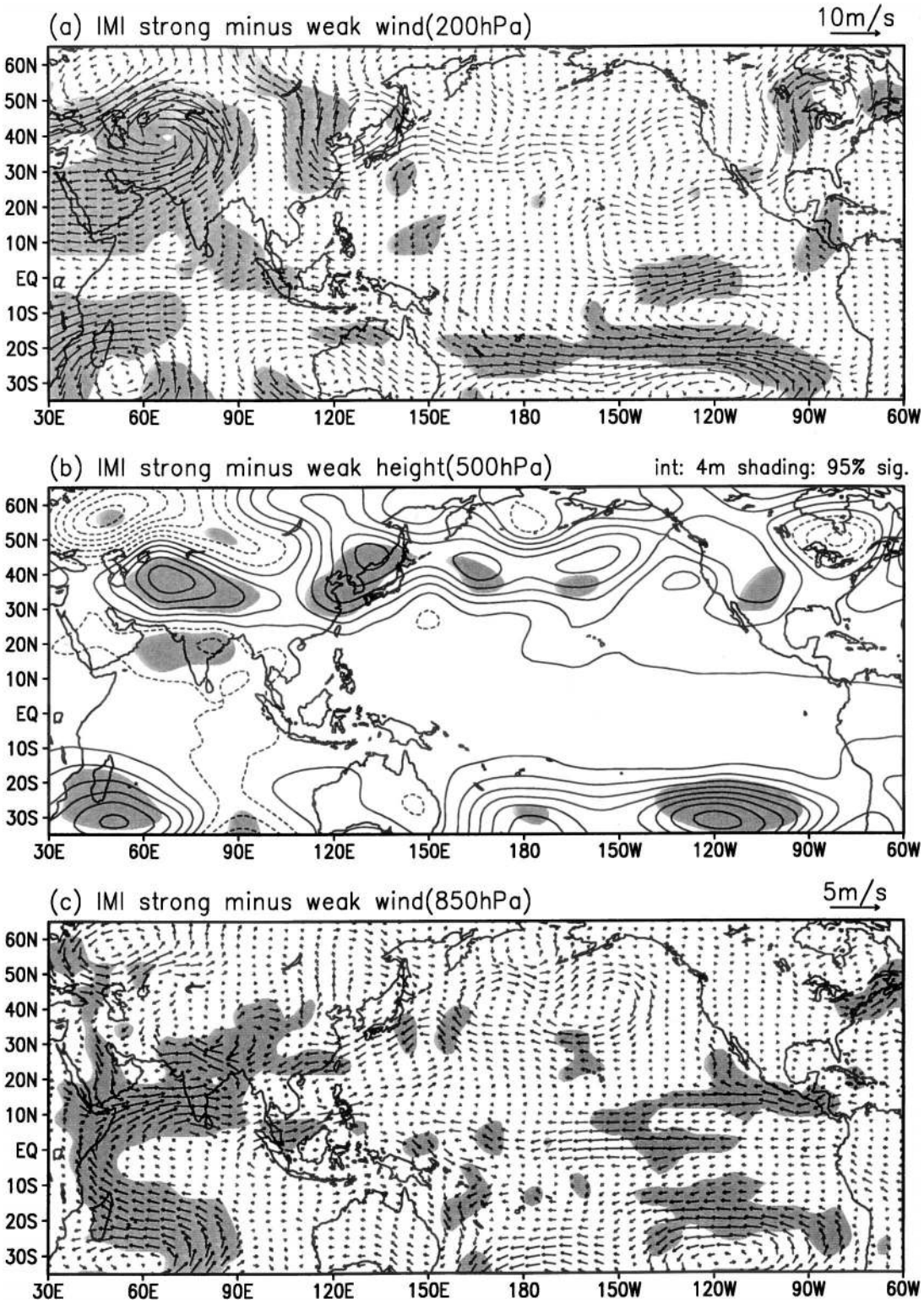

FIG. 8. Composite difference of (a) 200-hPa wind, (b) 500-hPa geopotential height, and (c) 850-hPa wind between strong and weak monsoon years with respect to the IMI. The contour interval for the height is 4 m. Shading denotes regions of difference at 95% confidence level. The wind scale is displayed at the upper right of (a), (b), and (c).

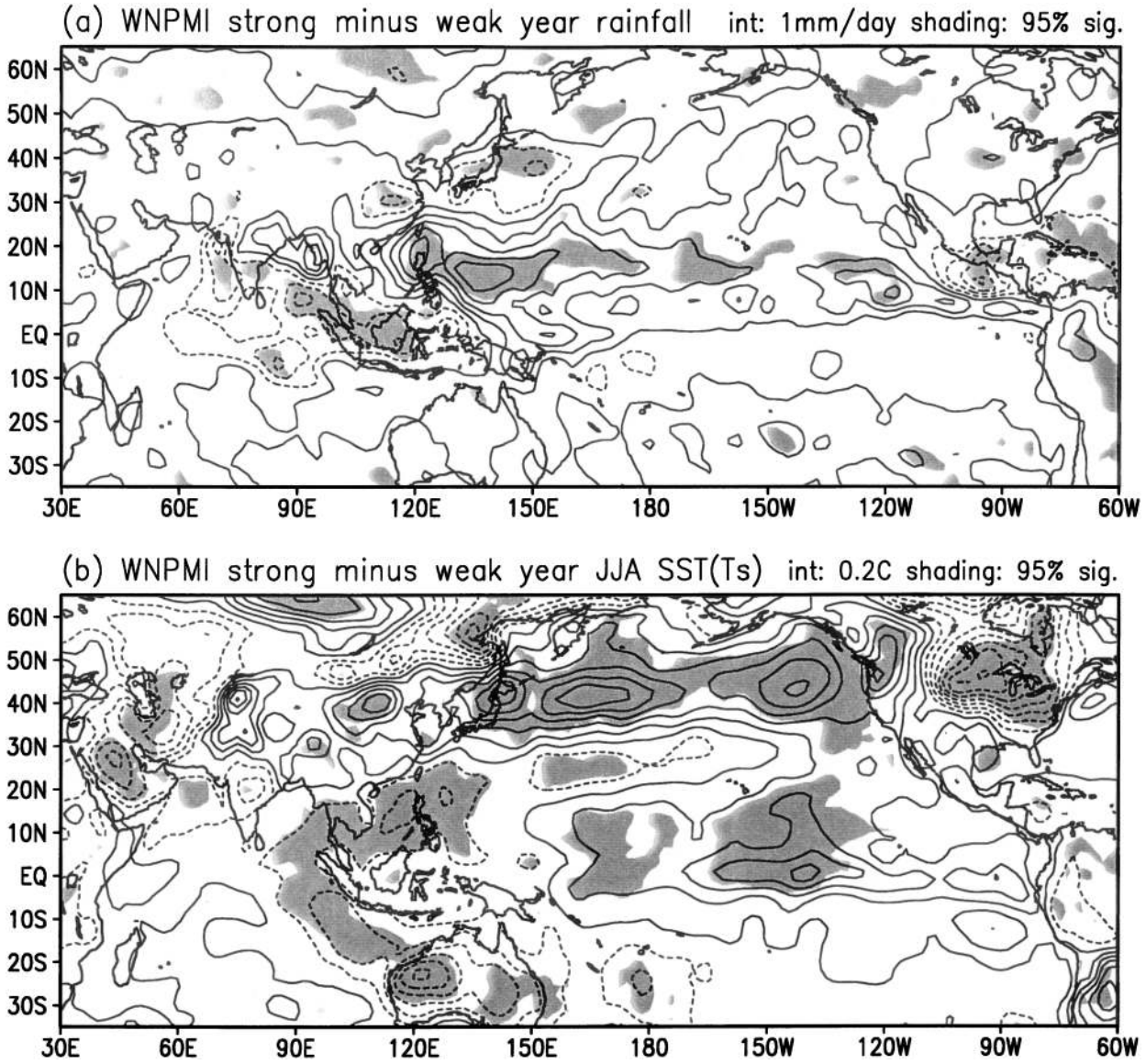

FIG. 9. The same as Fig. 7, but with respect to the WNPMI.

stream (as evidenced by the band structure in east Asia and WNP), which in turn excites optimum downstream circulation anomaly mode (such as the dipole pattern between the Gulf of Alaska–northwestern Canada and the Great Lakes–eastern Canada shown in Fig. 10). The other possible mechanism may be at work when the anomalous WNP heat source is centered north of 20°N so that the midlatitude westerlies allow the generation of the Rossby wave train to North America. The influences of midlatitude SST anomalies should not be overlooked. However, the North Pacific SST anomalies may be initially induced by wind anomalies associated with the WNP–EASM and atmospheric forcing from tropical eastern Pacific. These hypotheses deserve further exploration using numerical models.

6. Relationships between ENSO and the two Asian monsoon subsystems

To examine the relationships between the ISM and ENSO, we calculated the lag correlations of the Niño-3.4 (5°S–5°N, 170°–120°W) SST anomalies (used as an ENSO index) with reference to the ISM and WNPSM indices, the IMI and WNPMI (Fig. 11). In the last 50 years, the IMI has a statistically significant instantaneous negative correlation (-0.32) with Niño-3.4 SST anomaly in JJA(0) where the zero in brackets means the year during which ENSO develops (Fig. 11a). Since the Niño-3.4 SST anomaly normally reaches a maximum (or minimum) in boreal winter around December, the simultaneous negative correlation means an occurrence

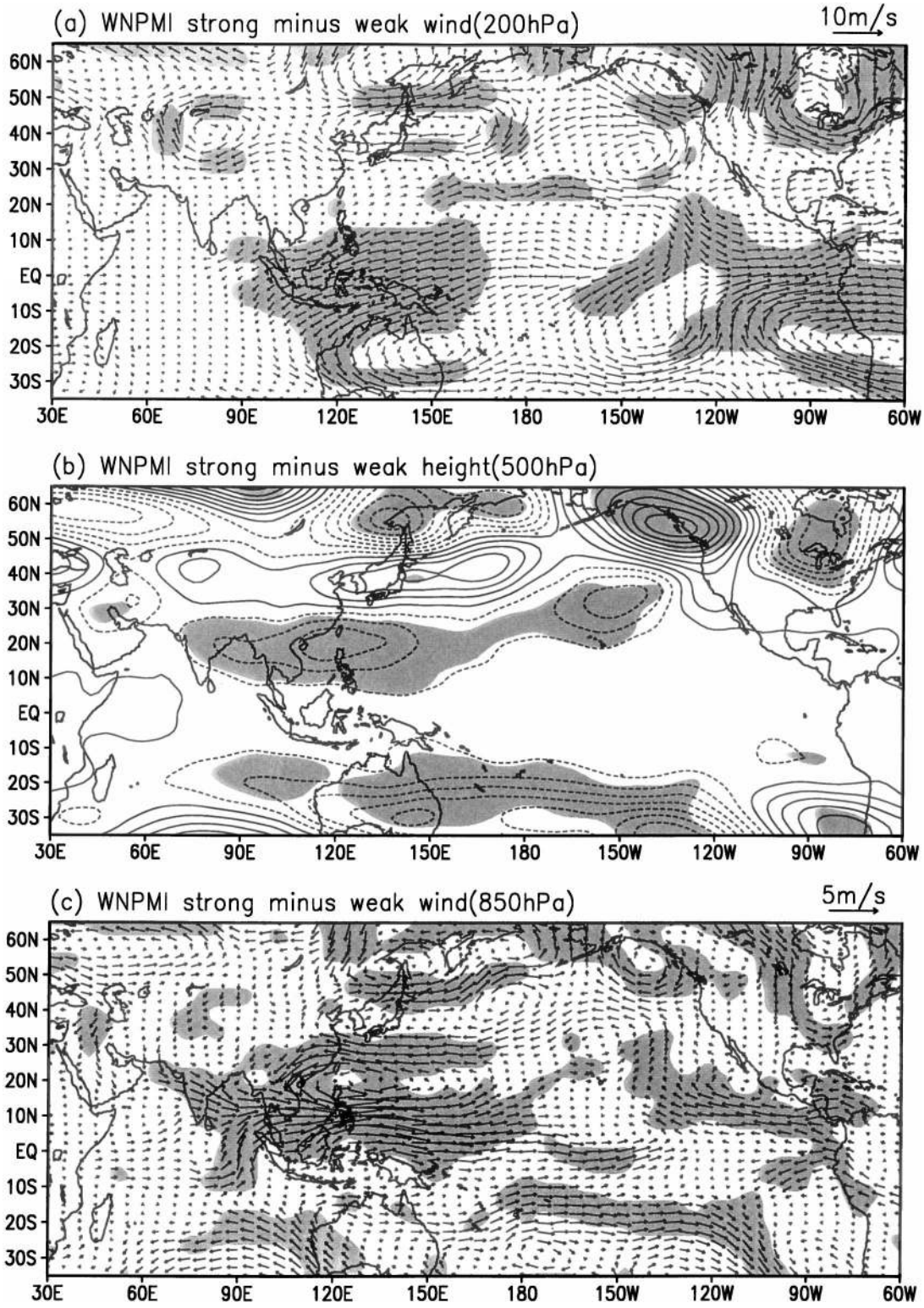

FIG. 10. The same as Fig. 8, but with respect to the WNPMI.

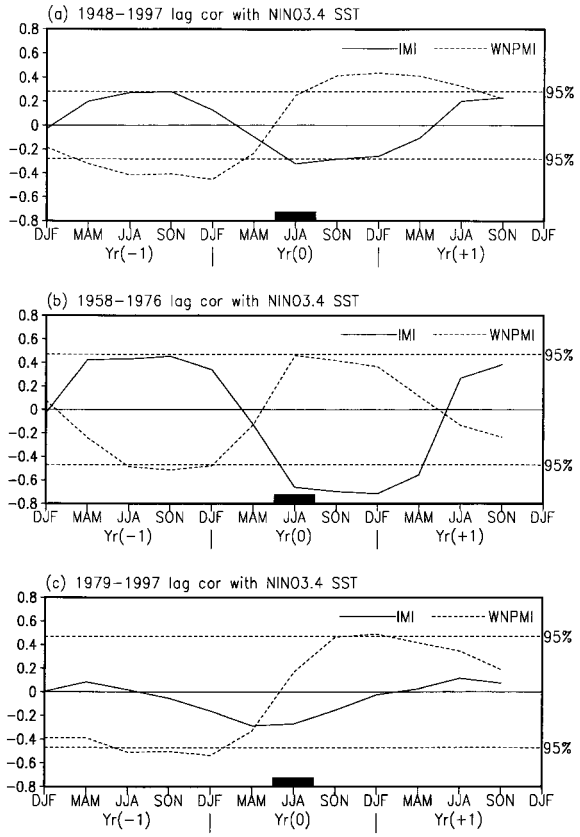

FIG. 11. Lag correlation of the seasonal mean Niño-3.4 SST anomalies with reference to the IMI (solid) and WNPSMI (dashed) at the summer of year (0) for the period of (a) 1948–97, (b) 1958–76, and (c) 1979–97. The dashed horizontal lines indicate correlation of 95% confidence level.

of a weak (strong) ISM in a *developing* El Niño (La Niña). This concurrent correlation also implies that ENSO is not a predictor for the ISM, nor can the ISM be used to predict ENSO. Inspection of the temporal evolution of the anomalous field confirms that *a strong ISM is preceded by an ENSO transition to a La Niña in the preceding spring, MAM(0)*. Similarly, a weak ISM is preceded by an ENSO transition to an El Niño. Therefore, the precursors in the tropical Pacific anomalies prior to ISM are extremely ambiguous.

The discrepancy between the correlation obtained here and that by Yasunari (1990) and Kirtman and Shukla (2000) may be accounted for by a dramatic change of the ISM–ENSO relationship in the late 1970s which coincides with the climate shift in the Pacific Ocean (Nitta and Yamada 1989; Trenberth 1990) and with a change of the El Niño properties (Wang 1995). During the pre-1977 period, the IMI correlates with Niño-3.4 SST anomaly simultaneously as well as with a lead of one or two seasons (Fig. 11b), in agreement with Yasunari's result. The correlation coefficient is approximately -0.7. The lead of a strong (weak) ISM to a La Niña (an El Niño), however, does not necessarily mean that a weak ISM causes an El Niño. Since the coupled ocean–atmosphere processes intrinsic to the tropical Pacific can lock the ENSO mature phase to the end of a calendar year (Tziperman et al. 1998; Clarke and Shu 2000; An and Wang 2000), the aforementioned ISM–ENSO relationship can be alternatively interpreted as a preferred occurrence of a weak ISM in the developing phase of an El Niño.

The negative ISM–ENSO correlation found for the period of 1958–76 has substantially weakened during the last two decades (Fig. 11c). This agrees with the previous findings of Shukla (1995) and Kumar et al. (1999). Notice that the ISM variability is relatively strong during the 1960s and 1970s and weak during the last two decades (Fig. 3b). It seems that a strong ENSO–ISM relationship is associated with large variability of the ISM. This supports the results obtained by Torrence and Webster (1999) who presented evidence of coherent multidecadal changes in the variance of both the all-Indian monsoon rainfall and Niño-3 SST anomaly.

The WNPMI in JJA(0) is significantly correlated with Niño-3.4 SST anomaly in the preceding winter, DJF(-1/0), with a negative correlation coefficient of -0.45 for the 50-yr period (Fig. 11a). This means that a weak (strong) WNPSM tends to occur in the summer *after* the mature phase of warm (cold) ENSO. Since the EASM rainfall in the mei-yu/baiu region tends to be in a phase opposite to that of the WNPSM rainfall, the above relationship also means that an above (below) normal EASM tends to occur in the summer right *after* a mature phase of El Niño (La Niña). This agrees with the Chinese meteorologists' experiences (Ye and Huang 1996). *The Niño-3.4 SST anomaly variation is an effective precursor for the WNP–EASM with a two-season lead.*

A weak WNPSM is not only preceded by the mature phase of a warm event in the preceding winter, but also tends to be followed by a cold state in the equatorial central-eastern Pacific during the ensuing fall, SON(0), and winter, DJF(0/1). This can be seen from its significant positive lag correlation with Niño-3.4 SST anomalies during SON(0) and DJF(0/1) (Fig. 11a), which suggests that *a weak WNPSM tends to lead a cold state in the equatorial eastern-central Pacific*. Note, however, this correlation explains about 17% of the variance and is dominated by a small number of strong (cold) warm events. The lag correlation pattern between WNPMI and ENSO index suggests that consecutive occurrence of development and decay phases of ENSO cycles associated with some strong warm events may yield a tendency of an isolated biennial signal, as suggested by Lau and Wu (2001). This, however, does not mean a continuous biennial oscillation.

In contrast to the ISM, the relationship between the WNPSM and ENSO appears to be much more steady in the last 50 years. As shown by the dotted curves in Figs. 11b and 11c, the lag correlation pattern in 1958–76 and 1979–97 is quite similar. Only a subtle change

occurs in the timing of the maximum positive correlation. In the pre-1977 epoch, the largest positive correlation is in the summer, whereas in the post-1977 epoch, it is in the winter following the summer monsoon.

7. Discussion

Why do the ISM and WNPSM exhibit differing interannual variations? The regionality of the Asian monsoon variability is in part due to spatial distribution of the thermal contrast between the ocean and continent. Over India, the *meridional* land–sea thermal contrast and thermal effects of the elevated Tibetan Plateau reinforce the interhemispheric thermal contrast resulting from differential solar radiation. As such, the Indian monsoon is extremely energetic. Over east Asia and its adjacent marginal seas, however, an east–west land–sea thermal contrast dominates, which tends to induce a zonal pressure difference between the Asian continental low and WNP subtropical high. In conjunction with the influence of the north–south differential solar forcing, the WNP subtropical high, along with the WNP monsoon trough to its southwest and the subtropical front to its northwest, controls the monsoon in east Asia and the WNP. From their geographic setting relative to the continent–ocean distribution, one would expect that the variability of the Indian and WNP monsoons might be dissimilar.

The ISM and the WNP–EASM are driven in part by two major convective heat sources. In summer, the two centers are anchored primarily in the Bay of Bengal and the Philippine Sea, respectively. The changes in intensity and location of the two convection regions have fundamental impacts on the variability of the two monsoon subsystems. Note that the convection in the WNP is more directly affected by the Pacific SST anomaly than is the convection over the Bay of Bengal. In addition, the ways by which ENSO affects the two convective heat sources differ (as will be discussed in the following two paragraphs). Therefore, the interannual variations of the ISM and WNPSM could be very different.

ENSO warming may affect the ISM through a longitudinal shift of the upward branch of the Walker circulation with implied additional subsidence over the Eastern Hemisphere (e.g., Palmer et al. 1992). This large-scale modulation and the complementary cooling in the western Pacific may shift the latitudinal position of the ITCZ in the eastern Indian and western Pacific Ocean, which would influence summer monsoon circulation in south Asia and WNP (Ju and Slingo 1995; Soman and Slingo 1997). As far as regional monsoon systems are concerned, the mechanisms through which the ocean affects monsoons are more complicated and subtle. For the ISM, the evidence presented by Lau and Nath (2000), based on analysis of results of numerical experiments with the Geophysical Fluid Dynamics Laboratory general circulation model, indicates that during a warm ENSO, the ISM trough weakens due to existence of equatorially symmetric Rossby waves (low-level high-pressure anomalies) excited by suppressed convection over the western pole of the Walker circulation. On the other hand, the reduced intensity of the ISM leads to a heat gain in the surface water of the Arabian Sea and the Bay of Bengal due to increased downward solar radiation and reduced evaporation cooling. The subsequent warming and the resulting SST gradients in turn force an anomalous atmospheric circulation that enhances the ISM. Therefore, the local air–sea interaction provides a negative feedback, which partially offsets the monsoon anomalies initially caused by remote ENSO forcing. This may in part account for the tantalizing ISM–ENSO relation.

As to the mechanism by which ENSO affect WNPSM and EASM, Wang et al. (2000) proposed that the in situ air–sea interaction in the WNP plays a key role. In the following we explain why a weak WNPSM (strong EASM) occurs in the decay phase of ENSO warm episodes, and the opposite is true for a strong WNPSM. Prior to a mature phase of an ENSO warming, a low-level anomalous anticyclone forms over the Philippine Sea. The anticyclone is then maintained until the following early summer by the following positive in situ air–sea feedback. In the eastern (western) part of the anomalous anticyclone, the anomalous northeast (southwest) winds increases (reduces) the total wind speed, thus enhancing (reducing) evaporative and entrainment cooling, leading to negative (positive) SST anomalies located to the east (west) of the anticyclone. The negative SST anomalies to the east of the anticyclone would in turn favor enhancement of the anticyclone through reducing convective latent heat release and exciting westward-propagating Rossby waves. This positive feedback is critical for maintaining the atmospheric anomalies to the ensuing summer. The southwesterly anomalies in the west side of the persistent Philippine Sea anticyclonic anomalies bring a warmer and wetter than normal winter and spring to the east Asian monsoon frontal zone and provide a prolonged impact on the ensuing early summer mei-yu/baiu. The devastating 1998 floods in the Yangtze River valley can be in part attributed to the delayed impact of the 1997 warm ENSO event.

The ISM exhibits a stronger biennial rhythm than the WNPSM. Positive SST anomalies in the northern Indian Ocean resulted from a weak ISM in the preceding year appear to persist through the winter preceding a strong ISM (figures not shown). This suggests that a weak ISM may lead to a strong one in the following year by exerting anomalous forcing into adjacent ocean that, in turn, is maintained by the ocean and feeds back to the atmosphere later. Chang et al. (2000) have explained how the Indian Ocean SST anomalies persist from boreal fall to the following spring. In the Eastern Hemisphere, both the atmosphere–ocean interaction (Nicholls 1978; Clarke et al. 1998; Chang and Li 2000) and at-

mosphere–ocean–land interaction (Meehl 1994, 1997) may support the biennial oscillation that dominates the interannual variation of the ISM.

The WNPSM–ENSO relationship does not show significant interdecadal variations, but the ISM–ENSO relation has experienced a remarkable weakening since the late 1970s. An obvious reason to account for this difference is that the WNPSM is more directly coupled with the eastern-central Pacific SST variation and its fluctuations occur primarily following peak phases of ENSO cycle. The delayed impacts of ENSO on the WNPSM and EASM explained by Wang et al. (2000) appear to be robust enough to resist other influences on longer timescales, such as interdecadal variations. On the other hand, the ISM variability is affected not only by ENSO but is also directly forced by the warm pool (tropical Indian and western Pacific) SST anomalies and Eurasian land surface anomalies, as well as local ocean–atmosphere–land interaction (e.g., Meehl 1994; Lau and Nath 2000). Thus, the ISM–ENSO relation is more fragile and vulnerable to the influences on decadal timescales. The present study shows that since the late 1970s the variance of the ISM has decreased, while that of the WNPSM has increased. In addition, the Webster and Yang index has an insignificant correlation coefficient (-0.12) with the WNPMI during 1958–77, but develops a significant correlation coefficient (0.45) after the late 1970s. This suggests that the broadscale Asian monsoon circulation may be controlled by the latent heat source over the WNP during the last two decades. This evidence seems to indicate that during the last two decades, ENSO conveys its impact on the Asian monsoon more via the WNP rather than via the Walker circulation, which may change the subtle ISM–ENSO relationship. Further studies are necessary to fully understand the interdecadal change of the ISM–ENSO relationship.

This study focused on the differences between the ISM and WNP–EASM. Distinguishing the differences is important in view of their distinct relations with ENSO and the different responses of midlatitude circulation to the heating in association with the ISM and WNPSM. However, the weak correlation between the IMI and WNPMI does not mean that the two monsoons are independent. Depending on the interfering or combining effects of remote and local forcing, the ISM and WNPSM can have different relation in different years. They also may interfere with each other through circulation changes.

8. Conclusions

The strength of the Asian summer monsoon is associated with intensities of two major convective heat sources centered primarily over the Bay of Bengal and Philippine Sea. The two heat sources exhibit distinct interannual variations and affect, respectively, the ISM and the WNPSM. Thus, two dynamic indices, which represent principal modes of the low-level circulation variability of the ISM and WNPSM, are proposed to measure their respective large-scale variability.

Variations of the ISM and WNPSM display remarkable differences. The ISM has a dominant timescale of about 30 months, whereas the WNPSM shows two preferred timescales: one at the low-frequency ENSO timescale (about 50 months), and the other around 16 months. The biennial rhythm in the WNPSM is weaker than that of the ISM. Figures 12a and 12b present two schematic diagrams that highlight, based on the composite results shown in Figs. 7–10, major rainfall and circulation anomalies associated with a strong ISM and a strong WNPSM, respectively. A strong ISM is characterized by 1) increased rainfall over India and the Bay of Bengal, 2) an enhanced low-level cross-equatorial gyre over the tropical Indian Ocean that connects with a deeper ISM trough to its north and a strengthened Mascarene high to its south, and 3) enhanced upper-level Tibetan Plateau and Mascarene highs and associated easterly anomalies over tropical Africa and the Indian Ocean. This anomalous circulation pattern suggests a strengthening of the entire ISM circulation system described by Krishnamurti and Bhalme (1976). A strong WNPSM features 1) increased rainfall over the South China Sea and WNP (8°–20°N, 110°–180°E) with a suppressed convective zone extending from Borneo to southern India, 2) a low-level elongated cyclonic circulation anomaly in the subtropical WNP (centered at 20°N and extending from 100° to 170°E) and an elongated anticyclonic anomaly along 35°N extending from 110°E to the date line, and 3) enhanced upper-level divergence over the Philippine Sea and associated easterlies and southward cross-equatorial flows over the Maritime Continent connected to an enhanced Australian high. Corresponding to a strong WNPSM, deficient rainfall occurs in the east Asian subtropical monsoon front extending from the lower reach of the Yangtze River valley to Japan. Thus, a strong WNPSM implies a suppressed mei-yu/baiu over east Asia, indicating a strong coupling between the WNPSM and EASM circulations. The circulation anomalies associated with an enhanced WNPSM suggest a strengthening of the entire WNP–EASM system visualized by Tao and Chen (1987).

Strong (weak) ISM tends to occur in developing phases of ENSO cold (warm) episodes, especially for the period before the late 1970s. As such, *precursory* signals over the tropical Pacific Ocean in the preceding spring are hardly detectable. Any effort searching for precursors has to focus on local SST anomalies over the Indian Ocean and the anomalous conditions over the Eurasian continent. In sharp contrast, the WNP–EASM has large-amplitude precursory signals, because a strong (weak) WNPSM is often preceded by a mature phase of ENSO cold (warm) episode. Land surface anomalies might provide additional precursory signals. In fact we found that a warming over Mongolia in winter and spring precedes a strong WNPSM (figure not shown). We note also that

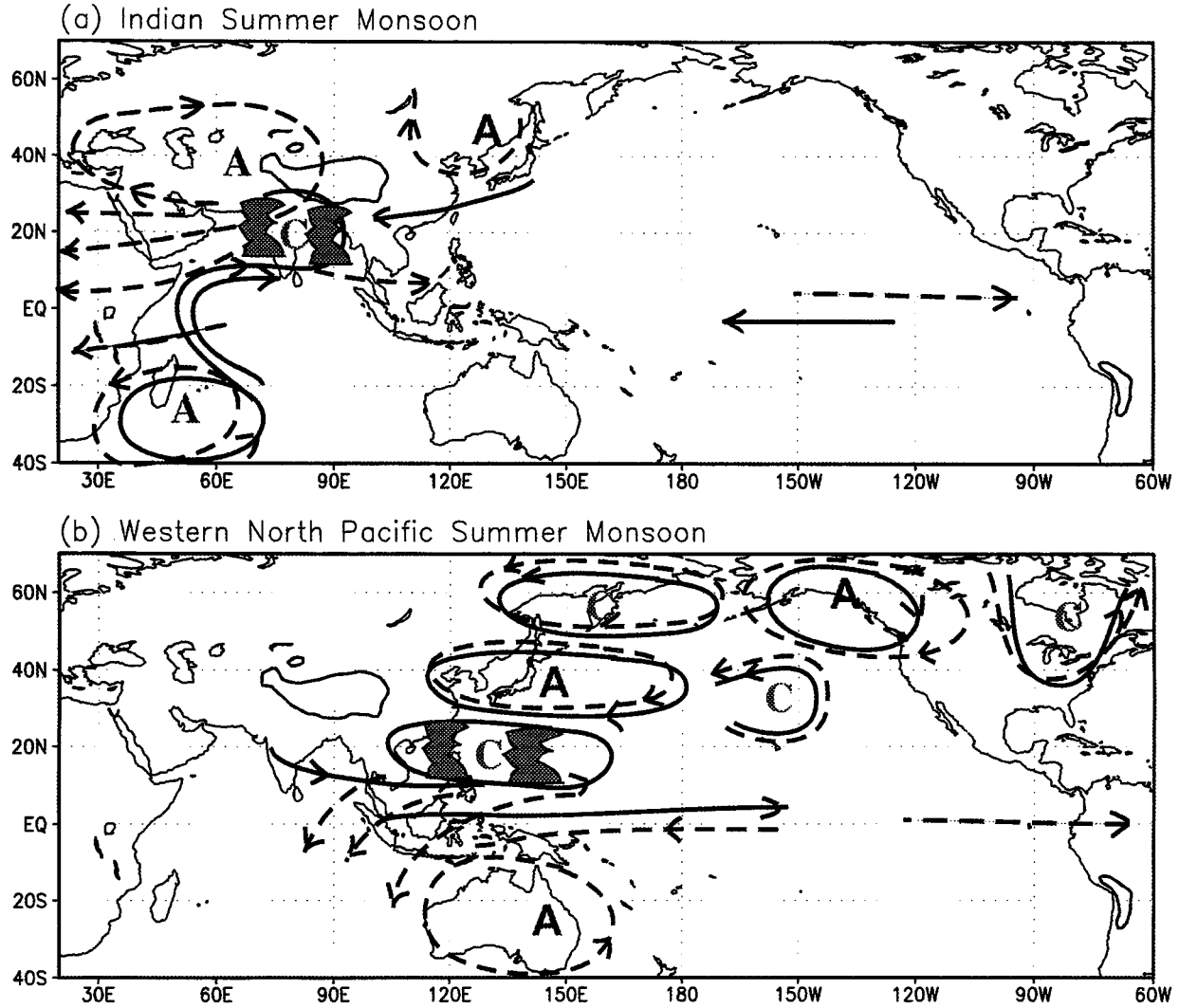

FIG. 12. Schematic diagrams showing the major circulation anomalies associated with (a) a strong Indian summer monsoon and (b) a strong western North Pacific summer monsoon. The lower-level and upper-level circulation anomalies are denoted by solid and dashed line, respectively. Letter ''A'' and ''C'' represent anticyclone and cyclone, respectively.

the WNPSM–ENSO relationship does not show significant interdecadal variations (Fig. 11), although the variance of the WNPSM has increased significantly since the late 1970s (Fig. 4b). However, the ISM–ENSO relation has remarkably weakened since the late 1970s concurrent with a decrease of ISM variance. In terms of ENSO–monsoon relationship, the WNPSM appears to be more predictable than the ISM.

The teleconnection patterns associated with ISM and WNPSM are also remarkably different. A strong Indian monsoon is associated with an enhanced South Pacific subtropical high and an anomalous anticyclone over northeast China. The latter indicates a linkage between the EASM and ISM. The variability of the EASM appears to be affected by both the WNPSM and ISM heat sources. An important finding is the teleconnection pattern between the WNPSM and North American summer climate. Suppressed WNPSM rainfall and convective latent heat release are shown to correlate with deficient summer rainfall in the U.S. Great Plains through an equivalent barotropic wave train. The wave train is associated with anomalous convection over the WNP and consists of five individual circulation anomaly cells with alternating signs. The physical processes by which the teleconnection pattern is established are under investigation.

Acknowledgments. The authors appreciate the comments on an earlier version of the manuscript made by Drs. Kemball-Cook, H. Annamalai, T. Yasunari, J. Chan, and an anonymous reviewer. This work is supported by NOAA OGP/Pacific Program.

REFERENCES

An, S.-I., and B. Wang, 2000: Interdecadal changes in the structure of ENSO mode and their relation to changes of ENSO frequency. *J. Climate,* **13,** 2044–2055.

Annamalai, H., J. M. Slingo, K. R. Sperber, and K. Hodges, 1999: The mean evolution and variability of the Asian summer monsoon: Comparison of ECMWF and NCEP–NCAR reanalyses. *Mon. Wea. Rev.,* **127,** 1157–1186.

Chang, C.-P., and T. Li, 2000: A theory for the tropical tropospheric biennial oscillation. *J. Atmos. Sci.,* **57,** 2209–2224.

——, Y. Zhang, and T. Li, 2000: Interannual and interdecadal variations of the East Asian summer monsoon and tropical Pacific SSTs. Part I: Roles of the subtropical ridge. *J. Climate,* **13,** 4310–4325.

Chen, L.-X., M. Dong, and Y.-N. Shao, 1992: The characteristics of interannual variations on the East Asian monsoon. *J. Meteor. Soc. Japan,* **70,** 397–421.

Chen, T.-C., and J.-H. Yoon, 2000: Interannual variation in Indochina summer monsoon rainfall: Possible mechanism. *J. Climate,* **13,** 1979–1986.

Clarke, A. J., and L. Shu, 2000: Quasi-biennial winds in the far western equatorial Pacific phase-locking El Niño to the seasonal cycle. *Geophys. Res. Lett.,* **27,** 771–774.

——, X. Liu, and S. V. Gorder, 1998: Dynamics of the biennial oscillation in the equatorial Indian and far western Pacific Oceans. *J. Climate,* **11,** 987–1001.

Gill, A. E., 1980: Some simple solutions for heat-induced tropical circulation. *Quart. J. Roy. Meteor. Soc.,* **106,** 447–462.

Goswami, B. N., V. Krishnamurthy, and H. Annamalai, 1999: A broad-scale circulation index for the interannual variability of the Indian summer monsoon. *Quart. J. Roy. Meteor. Soc.,* **125B,** 611–633.

Guo, Q., and J. Wang, 1988: A comparison of the summer precipitation in India with that in China (in Chinese). *J. Trop. Meteor.,* **4,** 53–59.

Huang, R., and Y. Wu, 1989: The influence of ENSO on the summer climate change in China and its mechanisms. *Adv. Atmos. Sci.,* **6,** 21–32.

Jiang, N., J. D. Neelin, and M. Ghil, 1995: Quasi-quadrennial and quasi-biennial variability in the equatorial Pacific. *Climate Dyn.,* **12,** 101–112.

Ju, J., and J. M. Slingo, 1995: The Asian summer monsoon and ENSO. *Quart. J. Roy. Meteor. Soc.,* **121,** 113–1168.

Kalnay, E., and Coauthors, 1996: The NCEP/NCAR 40-Year Reanalysis Project. *Bull. Amer. Meteor. Soc.,* **77,** 437–471.

Kirtman, B. P., and J. Shukla, 2000: Influence of the Indian summer monsoon on ENSO. *Quart. J. Roy. Meteor. Soc.,* **126,** 213–239.

Kripalani, R. H., and S. V. Singh, 1993: Large-scale aspects of India–China summer monsoon rainfall. *Adv. Atmos. Sci.,* **10,** 71–84.

——, and A. Kulkarni, 1997a: Climatic impacts of El Niño/La Niña on the Indian monsoon: A new perspective. *Weather,* **52,** 39–46.

——, and ——, 1997b: Rainfall variability over south-east Asia—Connections with Indian monsoon and ENSO extremes: New perspectives. *Int. J. Climatol.,* **17,** 155–1168.

Krishnamurthy, V., and B. N. Goswami, 2000: Indian monsoon–ENSO relationship on interdecadal timescale. *J. Climate,* **13,** 579–595.

Krishnamurti, T. N., and H. N. Bhalme, 1976: Oscillations of a monsoon system. Part I: Observational aspects. *J. Atmos. Sci.,* **33,** 1937–1954.

Kumar, K. K., B. Rajagopalan, and M. A. Cane, 1999: On the weakening relationship between the Indian monsoon and ENSO. *Science,* **284,** 2156–2159.

Lau, K.-M., 1992: East Asian summer monsoon rainfall variability and climate teleconnection. *J. Meteor. Soc. Japan,* **70,** 211–241.

——, and S. Yang, 1996: The Asian monsoon and predictability of the tropical ocean–atmosphere system. *Quart. J. Roy. Meteor. Soc.,* **122,** 945–957.

——, and H. Weng, 2001: Teleconnection linking summertime rainfall variability over North America and East Asia. *CLIVAR Exch.,* **5,** 18–21.

——, and H. T. Wu, 2001: Intrinsic coupled ocean–atmosphere modes of the Asian summer monsoon: A reassessment of monsoon–ENSO relationships. *J. Climate,* **14,** 2880–2895.

——, K.-M. Kim, and S. Yang, 2000: Dynamical and boundary forcing characteristics of regional components of the Asian summer monsoon. *J. Climate,* **13,** 2461–2482.

Lau, N.-C., and M. Nath, 2000: Impact of ENSO on the variability of the Asian–Australian monsoons as simulated in GCM experiments. *J. Climate,* **13,** 4287–4309.

Liu, X., and M. Yanai, 2001: Relationship between the Indian monsoon rainfall and the tropospheric temperature over the Eurasian continent. *Quart. J. Roy. Meteor. Soc.,* **127,** 909–938.

Matsuno, T., 1966: Quasi-geostrophic motions in the equatorial area. *J. Meteor. Soc. Japan,* **44,** 25–42.

Meehl, G. A., 1994: Coupled land–ocean–atmosphere processes and South Asian monsoon variability. *Science,* **266,** 263–267.

——, 1997: The South Asian monsoon and tropospheric biennial oscillation. *J. Climate,* **10,** 1921–1943.

Mooley, D. A., and J. Shukla, 1987: Variability and forecasting of the summer monsoon rainfall over India. *Monsoon Meteorology,* C. P. Chang and T. N. Krishnamurti, Eds., Oxford University Press, 26–59.

Nicholls, N., 1978: Air–sea interactions and the quasi-biennial oscillation. *Mon. Wea. Rev.,* **106,** 1505–1508.

Nitta, T., 1987: Convective activities in the tropical western Pacific and their impacts on the Northern Hemisphere summer circulation. *J. Meteor. Soc. Japan,* **65,** 165–171.

——, and S. Yamada, 1989: Recent warming of tropical sea surface temperature and its relationship to the Northern Hemisphere circulation. *J. Meteor. Soc. Japan,* **67,** 375–383.

Palmer, T. N., C. Brankoviz, P. Viterbo, and M. J. Miller, 1992: Modelling interannual variations of summer monsoons. *J. Climate,* **5,** 399–417.

Parthasarathy, B., K. R. Kumar, and D. R. Kothawaie, 1992: Indian summer monsoon rainfall indices: 1871–1990. *Meteor. Mag.,* **121,** 174–186.

Rasmusson, E. M., and T. Carpenter, 1983: The relationship between eastern equatorial Pacific sea surface temperature and rainfall over India and Sri Lanka. *Mon. Wea. Rev.,* **111,** 517–527.

Shen, S., and K.-M. Lau, 1995: Biennial oscillation associated with the East Asian summer monsoon and tropical sea surface temperatures. *J. Meteor. Soc. Japan,* **73,** 105–124.

Shukla, J., 1995: Predictability of the tropical atmosphere, the tropical oceans and TOGA. *Proc. Int. Conf. on the Tropical Ocean Global Atmosphere (TOGA) Programme, Vol. 2,* WCRP-91, Geneva, Switzerland, World Climate Research Programme, 725–730.

——, and D. A. Paolino, 1983: The Southern Oscillation and long-range forecasting of the summer monsoon rainfall over India. *Mon. Wea. Rev.,* **111,** 1830–1837.

Soman, M. K., and J. Slingo, 1997: Sensitivity of Asian summer monsoon to aspects of sea surface temperature in the tropical Pacific Ocean. *Quart. J. Roy. Meteor. Soc.,* **123,** 309–336.

Tao, S., and L. Chen, 1987: A review of recent research on the East Asian summer monsoon in China. *Monsoon Meteorology,* C.-P. Chang and T. N. Krishnamurti, Eds., Oxford University Press, 60–92.

Ting, M., and H. Wang, 1997: Summertime U.S. precipitation variability and its relation to Pacific sea surface temperature. *J. Climate,* **10,** 1853–1873.

Tomita, T., and T. Yasunari, 1996: Role of northeast winter monsoon on the biennial oscillation of the ENSO/monsoon system. *J. Meteor. Soc. Japan,* **74,** 399–413.

Torrence, C., and P. J. Webster, 1999: Interdecadal changes in the ENSO–monsoon system. *J. Climate,* **12,** 2679–2710.

Trenberth, K. E., 1990: Recent observed interdecadal climate changes in the Northern Hemisphere. *Bull. Amer. Meteor. Soc.,* **71,** 988–993.

Tziperman, E., M. A. Cane, and B. Blumenthal, 1998: Locking of El Niño peak time to the end of the calendar year in the delayed oscillator picture of ENSO. *J. Climate,* **11,** 2191–2203.

Walker, G. T., 1923: Correlation in seasonal variations of weather. VIII: A preliminary study of world weather. *Mem. Indian Meteor. Dep.,* **24,** 75–131.

——, 1924: Correlation in seasonal variations of weather. IV: A further study of world weather. *Mem. Indian Meteor. Dep.,* **24,** 275–332.

Wang, B., 1995: Interdecadal changes in El Niño onset in the last four decades. *J. Climate,* **8,** 267–285.

——, 2000: Reply. *Bull. Amer. Meteor. Soc.,* **81,** 822–824.

——, and Z. Fan, 1999: Choice of South Asian summer monsoon indices. *Bull. Amer. Meteor. Soc.,* **80,** 629–638.

——, R. Wu, and R. Lukas, 1999: Roles of the western North Pacific wind variation in thermocline adjustment and ENSO phase transition. *J. Meteor. Soc. Japan,* **77,** 1–16.

——, ——, and X. Fu, 2000: Pacific–East Asian teleconnection: How does ENSO affect East Asian climate? *J. Climate,* **13,** 1517–1536.

Webster, P. J., and S. Yang, 1992: Monsoon and ENSO: Selectively interactive systems. *Quart. J. Roy. Meteor. Soc.,* **118,** 877–926.

——, V. O. Magaña, T. N. Palmer, R. A. Thomas, M. Yanai, and T. Yasunari, 1998: Monsoons: Processes, predictability, and the prospects for prediction. *J. Geophys. Res.,* **103,** 14 451–14 510.

Weng, H., K.-M. Lau, and Y.-K. Xue, 1999: Multi-scale summer rainfall variability over China and its long-term link to global sea surface temperature variability. *J. Meteor. Soc. Japan,* **77,** 845–857.

Wu, R., and B. Wang, 2000: Interannual variability of summer monsoon onset over the western North Pacific and the underlying processes. *J. Climate,* **13,** 2483–2501.

Xie, P., and P. A. Arkin, 1997: Global precipitation: A 17-year monthly analysis based on gauge observations, satellite estimates, and numerical outputs. *Bull. Amer. Meteor. Soc.,* **78,** 2539–2558.

Yanai, T., and C. Li, 1994: Interannual variability of the Asian summer monsoon and its relationship with ENSO, Eurasian snow cover, and heating. *Proc. Int. Conf. on Monsoon Variability and Prediction,* Trieste, Italy, WMO, 27–34.

Yasunari, T., 1990: Impact of Indian monsoon on the coupled atmosphere–ocean systems in the tropical Pacific. *Meteor. Atmos. Phys.,* **44,** 29–41.

Ye, D.-Z., and R.-H. Huang, 1996: *Study on the Regularity and Formation Reason of Drought and Flood in the Yangtze and Huaihe River Regions* (in Chinese). Shandon Science and Technology Press, 387 pp.

Zhang, R., A. Sumi, and M. Kimoto, 1996: Impacts of El Niño on the East Asian monsoon: A diagnostic study of the '86/87 and '91/92 events. *J. Meteor. Soc. Japan,* **74,** 49–62.

——, ——, and ——, 1999: A diagnostic study of the impact of El Niño on the precipitation in China. *Adv. Atmos. Sci.,* **16,** 229–241.